Wen Zhou
Kristina Håkansson

Department of Chemistry, University of Michigan, Ann Arbor, MI, USA

Research Article

Electron detachment dissociation of fluorescently labeled sialylated oligosaccharides

We explored the application of electron detachment dissociation (EDD) and infrared multiphoton dissociation (IRMPD) tandem mass spectrometry to fluorescently labeled sialylated oligosaccharides. Standard sialylated oligosaccharides and a sialylated *N*-linked glycan released from human transferrin were investigated. EDD yielded extensive glycosidic cleavages and cross-ring cleavages in all cases studied, consistently providing complementary structural information compared with infrared multiphoton dissociation. Neutral losses and satellite ions such as C−2H ions were also observed following EDD. In addition, we examined the influence of different fluorescent labels. The acidic label 2-aminobenzoic acid (2-AA) enhanced signal abundance in negative-ion mode. However, few cross-ring fragments were observed for 2-AA-labeled oligosaccharides. The neutral label 2-aminobenzamide (2-AB) resulted in more cross-ring cleavages compared with 2-AA-labeled species, but not as extensive fragmentation as for native oligosaccharides, likely resulting from altered negative charge locations from introduction of the fluorescent tag.

1 Introduction

Glycosylation plays essential roles in a variety of cellular processes, including tumor growth and metastasis, immune response, and cell–cell communication [1–6]. Sialic acids (e.g. *N*-acetyl neuraminic acid, NeuAc) are an important family of sugars that contains a carboxylic acid at the C-1 position of the six-member sugar ring. Sialic acids are often found at the terminal positions of glycans and glycoconjugates and are involved in a large number of protein–glycan and glycan–glycan interactions in cellular processes, including intercellular adhesion, signaling, and microbial attachment [7]. Compared with proteomics and genomics, glycomic analysis faces unique challenges due to the

Correspondence: Professor Kristina Håkansson, Department of Chemistry, University of Michigan, 930 North University Avenue, Ann Arbor, MI 48109-1055, USA
E-mail: kicki@umich.edu
Fax: +1-734-615-3790

Abbreviations: 2-AA, 2-aminobenzoic acid; **2-AB,** 2-amino-benzamide; **CAD,** collision-activated dissociation; **DSLNT,** disialyl-lacto-*N*-tetraose; **EDD,** electron detachment dissociation; **IRMPD,** infrared multiphoton dissociation; **LSTb,** LS-tetrasaccharide b

nontemplate-driven biosynthesis and the highly diverse structures of glycans. In order to achieve thorough structural elucidation of glycans, monosaccharide composition, degree of branching (for branched glycans), linkage type, and anomeric configuration all need to be determined.

MS-based structural characterization of glycans is gaining popularity due to its high sensitivity and ability to perform high-throughput analysis [8–11]. Fourier transform ion cyclotron resonance (FT-ICR) MS is a powerful tool for the structural analysis of glycans benefiting from ultra-high mass accuracy and resolution, as well as compatibility with various MS/MS techniques [12–14]. While mass profiling of glycans can be obtained by MS, detailed structure elucidation requires MS/MS. Collision-activated dissociation (CAD) [15–17], infrared multiphoton dissociation (IRMPD) [18–20], high-energy CAD (heCAD) [21–23], electron capture dissociation (ECD) [24–28], electron detachment dissociation (EDD) [29–34], negative electron transfer dissociation (NETD) [35], 157 nm photodissociation [36–38], and electron-induced dissociation (EID) [39] have all been applied for glycan structural characterization.

During IRMPD, precursor ions are irradiated by an IR laser (typically 10.6 μm CO_2 laser). Multiple photons are

---

absorbed and the corresponding energy is redistributed over all precursor ion vibrational modes [40, 41]. Compared with CAD, IRMPD is more advantageous for glycan structural analysis because of its ability to readily generate secondary fragmentation, which provides higher fragmentation efficiency, particularly for large glycans [18]. EDD was first introduced in 2001 for the characterization of peptide anions [42]. During EDD, polyanions are irradiated with $> 10\,eV$ energy electrons. Electron detachment occurs to generate charge-reduced species, followed by subsequent radical-driven fragmentation [43]. Our lab previously showed that EDD provides complementary structural information for model oligosaccharides and sialylated *N*-glycans compared with IRMPD [34, 44]. Amster and coworkers investigated the fragmentation behavior in EDD of glycosaminoglycans, and found that EDD yielded extensive glycosidic and cross-ring cleavages, whereas CAD and IRMPD mostly resulted in glycosidic cleavages [29–33, 45]. EDD could also be utilized to differentiate the isomers glucuronic acid and iduronic acid [29]. The combination of EDD and IRMPD/CAD is a highly valuable tool for structural characterization of carbohydrates, particularly acidic carbohydrates in negative-ion mode, due to the ability to provide complementary structural information.

Fluorescent labeling of glycans is frequently employed prior to MS for several reasons. First, introduction of a hydrophobic label to hydrophilic glycans improves ionization efficiency [46]. Second, fluorescent labels enable UV- or fluorescence-based detection in high-performance liquid chromatography (HPLC), and also enhance glycan retention on reversed-phase (e.g. C_{18}) columns [47–50]. Native glycans often exhibit poor retention, whereas derivatized glycans can be separated and identified with C_{18} columns [51]. In addition, recent studies have demonstrated that quantitation of glycans can be obtained by utilizing stable isotope labeling [52–54]. The most commonly used labeling method is reductive amination. The primary amine of the label reacts with the aldehyde group of the glycan to generate a Schiff base intermediate, which is then stabilized through reduction to form a secondary amine [55]. 2-Aminobenzoic acid (2-AA), 2-aminobenzamide (2-AB), 2-aminopyridine (2-AP), and 5-amino-2-naphthalenesulfonic acid (ANSA) are some of the commonly utilized fluorescent labels [56–68].

It has been previously reported that labels may change MS fragmentation behaviors of glycans [48, 50, 69]. For neutral glycans and labeled glycans which do not contain acidic groups, positive-ion mode analysis is frequently employed. 2-AB-tagged oligosaccharides were examined in both protonated and sodiated forms by CAD, high-energy CAD, post-source decay (PSD), and ultraviolet photodissociation (UVPD) [59–61, 64, 70, 71]. Harvey reported that 2-AB labeling at the reducing end did not significantly alter fragmentation behavior of *N*-glycans in CAD [59]. Protonated species mostly produced B- and Y-type glycosidic cleavages, whereas sodiated species generated additional C-, and Y-type as well as cross-ring fragments [60, 71]. 355 nm ultraviolet photodissociation of fluorescently labeled sodi-

ated oligosaccharides resulted in efficient fragmentation, generating series of A- and C-ions, complementary to CAD [70]. 2-AB-labeled oligosaccharides were also analyzed in negative-ion mode MALDI-TOF/TOF-MS, demonstrating considerably different fragmentation patterns compared with positive-ion mode [63]. Various cross-ring fragments such as ^{1,3}A-type ions were observed, providing linkage information. In addition, fucose residues were stabilized in negative-ion mode analysis, which allowed improved fucosylation site determination [63]. Acidic glycans (e.g. sialylated glycans) or glycans with acidic labels (e.g. 2-AA) tend to produce abundant signals in negative-ion mode, which makes negative-ion mode analysis a highly favorable choice. 2-AA-labeled *N*-glycans mostly generate Y-type ions containing the reducing end and also some A-type cross-ring cleavages in negative-ion mode CAD [15]. Here, we investigate the fragmentation behaviors of fluorescently labeled sialylated oligosaccharides by EDD and IRMPD, and compare those with the fragmentation patterns of the corresponding underivatized species.

2 Materials and methods

2.1 Reagents

Disialyl-lacto-*N*-tetraose (DSLNT) and LS-tetrasaccharide b (LSTb) were purchased from V-labs (Covington, LA). Human apo-transferrin, 1,4-dithio-DL-threitol (DTT), iodoacetamide, 2-AA, 2-AB, boric acid, sodium acetate, and sodium cyanoborohydride ($NaCNBH_3$) were obtained from Sigma Chemical (St. Louis, MO). NH_4HCO_3, NH_4OH, methanol, acetonitrile, glacial acetic acid, dimethyl sulfoxide (DMSO), and formic acid were obtained from Fisher (Fair Lawn, NJ). Peptide-*N*-glycosidase F (PNGase F) was purchased from Calbiochem (Gibbstown, NJ).

2.2 Preparation of *N*-linked glycans

The glycoprotein was reduced in 5 mM 1,4-dithio-DL-threitol at 56°C for 45 min, alkylated by 15 mM iodoacetamide in the dark at room temperature for 1 h, and digested with peptide-*N*-glycosidase F (2 U) in 50 mM NH_4HCO_3 (pH = 8) overnight at 37°C.

2.3 Fluorescent labeling of oligosaccharides

Oligosaccharides (2 nmol) were dried down, reconstituted in 60 μL freshly prepared labeling reagent, and incubated at 80°C for 1 h (2-AA) or 65°C for 2 h (2-AB). For 2-AA labeling, labeling reagent was prepared by dissolving 30 mg 2-AA and 30 mg $NaCNBH_3$ in 1 mL methanol containing 4% sodium acetate w/v and 2% boric acid w/v. For 2-AB labeling, labeling reagent was 0.35 M 2-AB and 1 M $NaCNBH_3$ in a DMSO/glacial acetic acid mixture (7:3 v/v).

2.4 Purification of oligosaccharides

The fluorescently labeled oligosaccharides were purified by SPE-graphitized carbon cartridge (Alltech Associates, Deerfield, IL). For each sample, a carbon cartridge was washed with 0.1% v/v formic acid in 80% ACN/H_2O v/v, followed by deionized water. The solution containing labeled oligosaccharides was loaded and the cartridge was then washed by deionized water to remove salts and other contaminants. The glycans were eluted with 0.1% formic acid v/v in 20 or 40% acetonitrile/H_2O v/v. The solution was then dried down in a vacuum concentrator (Eppendorf, Hamburg, Germany) and reconstituted in 50% methanol, 0.1% NH_4OH v/v solution for MS analysis.

2.5 MS

All mass spectra were collected with an actively shielded 7 T FT-ICR mass spectrometer with a quadrupole front-end (APEX-Q, Bruker Daltonics, Billerica, MA), as described previously [72]. An indirectly heated hollow dispenser cathode was used to perform EDD [73]. IRMPD was performed with a vertically mounted 25 W, 10.6 μM CO_2 laser (Synrad, Mukilteo, WA). Samples were infused via an Apollo II electrospray ion source at a flow rate of 70 μL/h with the assistance of N_2 nebulizing gas. Following ion accumulation in the first hexapole for 50 ms, ions were mass selectively accumulated in the second hexapole for 1–6 s. Ions were then transferred through high-voltage ion optics and captured with dynamic trapping in an Infinity ICR cell [74]. The accumulation sequence up to the ICR cell fill was looped three times to optimize precursor ion signal to noise ratio (S/N). For EDD, the cathode heating current was kept at 2.0 A and the cathode voltage was pulsed to a bias voltage of −30 to −35 V [34] for 1 s. An extraction lens located in between the cathode and the ICR cell was kept −0.8 to −1.0 V higher than the cathode bias voltage. An electron current of a few microamperes is optimum for EDD [75]. IRMPD was performed with a laser power of 10 W with firing times ranging from 0.25 to 1 s.

2.6 Data analysis

All mass spectra were acquired with XMASS software (Bruker Daltonics) with 256 data points from m/z 100 to 2000 and summed over 60–100 scans. Data processing was performed with MIDAS software [76]. Data were zero filled once, Hanning apodized, and exported to Microsoft Excel for internal frequency-to-mass calibration with a two-term calibration equation [77]. Product ion spectra were interpreted with the aid of the web application GlycoFragment (http://www.glycosciences.de/tools/GlycoFragments/) [78]. Product ions were not assigned unless they were at least three times the noise level.

3 Results

MS/MS spectra of oligosaccharides mainly contain two types of bond cleavages: glycosidic cleavages which occur between monosaccharide residues, and cross-ring cleavages occurring across sugar rings [79]. Glycosidic cleavages provide structural information regarding monosaccharide composition, whereas cross-ring cleavages aid the determination of linkage type. EDD and IRMPD fragmentation patterns of the 2-AA- and 2-AB-labeled sialylated oligosaccharides DSLNT and LSTb, and an *N*-glycan released from human transferrin were investigated. Structures of 2-AA and 2-AB are shown in Fig. 1.

3.1 DSLNT

DSLNT is a branched di-sialylated oligosaccharide with the composition Neu5Acβ3Galβ3(Neu5Acβ6)GlcNAcβ3-Galβ4Glc. Negative-ion mode IRMPD of 2-AB-labeled DSLNT resulted in an almost complete series of Y-ions, all containing the fluorescent label (Fig. 2A), similar to the fragmentation patterns from MALDI-post-source decay of 2-AB-labeled oligosaccharides [61]. $Y_{4\alpha(3\beta)}$ ($m/z = 1117.4$), corresponding to loss of either sialic acid, was the most abundant species among the product ions, illustrating the gas-phase lability of sialic acids. No cross-ring fragments were found, thus precluding acquisition of linkage information. EDD of doubly deprotonated 2-AB-labeled DSLNT resulted in extensive fragmentation (Fig. 2B). All product ions were singly charged, which may arise from two different fragmentation mechanisms: either via direct fragmentation of activated precursor ions, or via the charged reduced radical ions generated after electron detachment [32]. Glycosidic cleavages between every neighboring monosaccharide were observed, along with five cross-ring cleavages, including $^{0,2}A$-, $^{1,5}A$-, $^{0,2}X$-, and $^{1,5}X$-type ions. $^{0,2}X$- and $^{1,5}X$-type ions are generally not present in CAD/IRMPD spectra, but they have been observed from high-energy CAD, laser-induced dissociation (LID) of sodiated fluorescently labeled oligosaccharides [63, 69], and from EDD of underivatized oligosaccharides and GAGs [30, 32, 34]. Among all the product ions, $C_{1\alpha(1\beta)}$ ($m/z = 308.1$), corresponding to loss of one sialic acid, was the most abundant species. CO_2 loss from the charge-reduced species, glycosidic fragments, and from cross-ring fragments was frequently observed, presumably originating from the carboxylic acid of the sialic acids. This neutral loss complicates the spectral appearance. Several satellite peaks, such as C−2H, Y−2H, and Y−16 Da (or Z+2H) [34] were
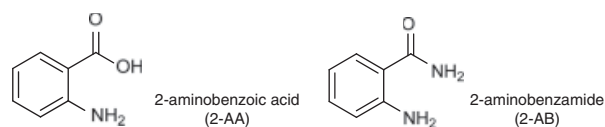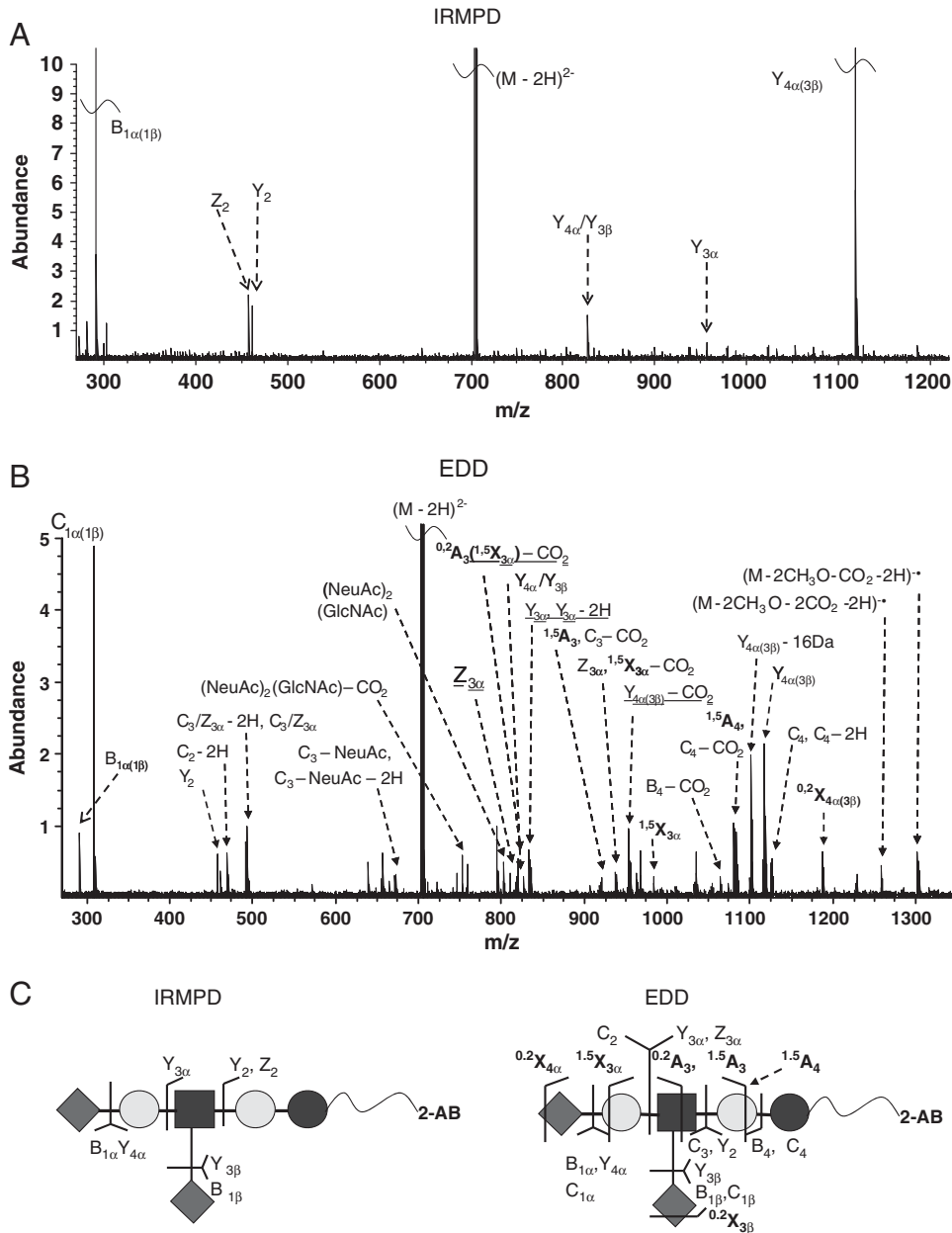

Figure 1. Structures of 2-AA and 2-AB.

Figure 2. (A) IRMPD (80 scans, 0.8 s at 10 W) and (B) EDD (80 scans, 1 s irradiation, cathode bias, –30 V) spectra of doubly deprotonated 2-AB-labeled DSLNT ($m/z = 703.75$). Cross-ring fragments are highlighted in bold and reducing end product ions lacking 2-AB are underlined in the spectra. All product ions are singly charged. Fragmentation patterns from IRMPD and EDD are shown in (C).

also found in the spectra. Such ions were observed only in EDD, indicating that they may arise from radical-driven fragmentation pathways [30]. Compared with IRMPD, EDD produced additional structural information including both glycosidic and cross-ring cleavages, rendering EDD a highly valuable and promising tool for structural characterization of fluorescently labeled oligosaccharides in negative-ion mode.

MS/MS of 2-AA-labeled DSLNT is shown in Fig. 3. Compared with 2-AB-labeled species, 2-AA-labeled DSLNT readily generated abundant signal in negative-ion mode. In order to compare the fragmentation behaviors, shorter ion accumulation time was chosen for 2-AA-tagged species to yield the same precursor ion abundance. IRMPD of 2-AA-labeled DSLNT mostly resulted in Y-ions containing the fluorescent tag, which could aid the determination of monosaccharide composition and "sequence" of the oligo-saccharide (Fig. 3A). Again, no cross-ring cleavages were produced. However, in contrast to 2-AB-labeled DSLNT, the $Y_{4\alpha(3\beta)}$ product ion, corresponding to loss of one sialic acid, does not dominate the IRMPD spectrum of 2-AA-labeled DSLNT. Instead, $Y_{4\alpha}/Y_{3\beta}$, corresponding to loss of both sialic acids, is dominant and $Y_{3\alpha}/Y_{3\beta}$ product ions, which also have lost both sialic acids and an additional galactose
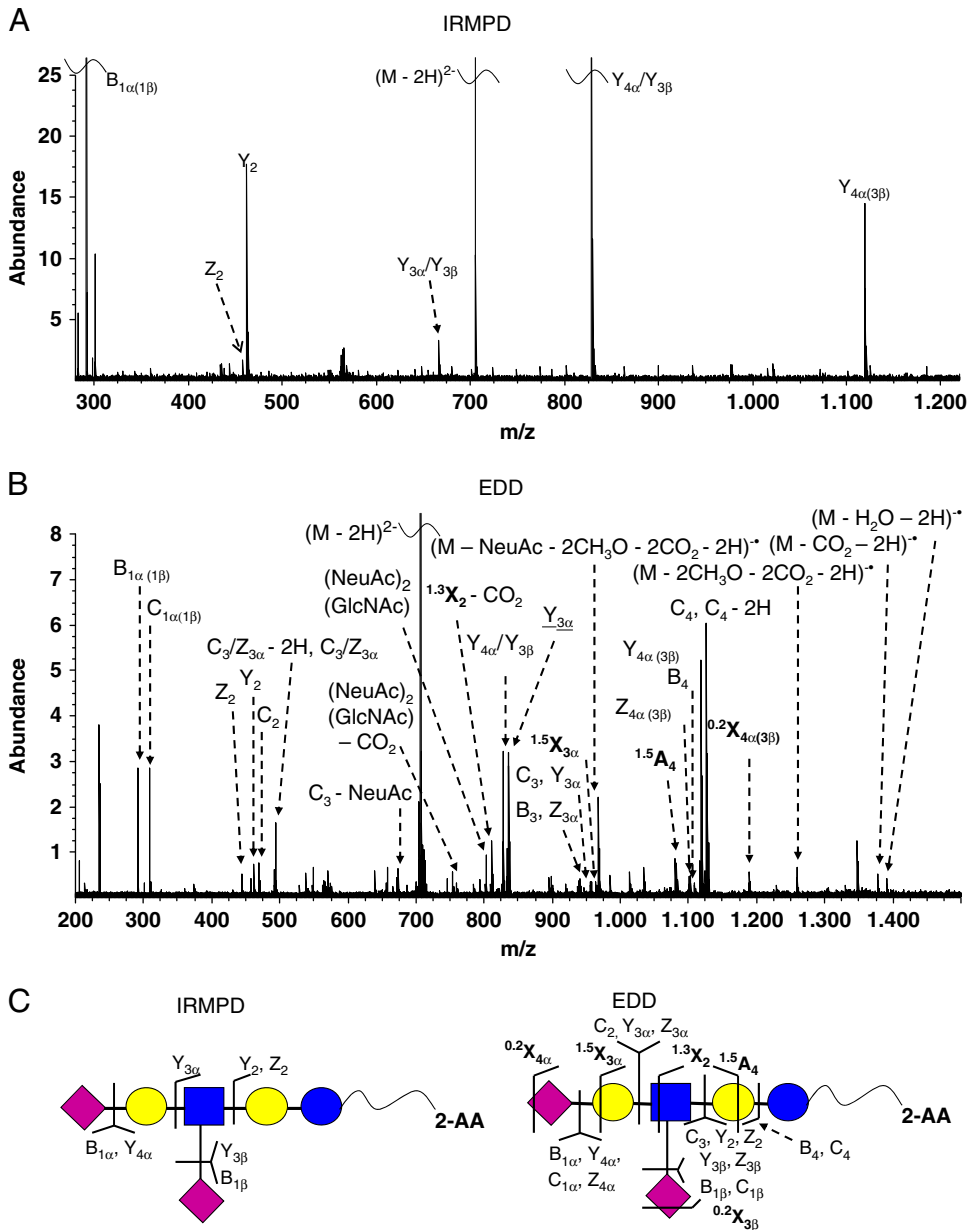
Figure 3. (A) IRMPD (80 scans, 1 s at 10 W) and (B) EDD (80 scans, 1 s irradiation, cathode bias, −30 V) spectra of doubly deprotonated 2-AA-labeled DSLNT ($m/z = 704.24$). Cross-ring fragments are highlighted in bold and reducing end fragment ions lacking 2-AA are underlined in the spectra. All product ions are singly charged. Fragmentation patterns from IRMPD and EDD are shown in (C).

residue, are observed. The latter product was not detected in IRMPD of 2-AB-labeled DSLNT. The higher abundance of these two product ions for the 2-AA-labeled species is likely due to the higher probability of retaining charge on the reducing end due to the acidic label.

EDD of 2-AA-labeled DSLNT demonstrated similar fragmentation compared with the 2-AB-labeled species (Fig. 3B). Thirteen glycosidic and four cross-ring cleavages were observed, including $^{1,5}A$-, $^{0,2}X$-, $^{1,3}X$-, and $^{1,5}X$-type ions. All product ions were singly charged. Extensive neutral loss (CO_2, CH_3O, and H_2O) from the charged reduced species and from glycosidic fragments, and internal fragments were observed in the EDD spectrum. Similar to Fig. 2B, satellite ions such as C_4-2H were found. Their absence

in the IRMPD spectrum of the same species suggests that such ions may originate from radical-driven fragmentation, or from electronic excitation. Compared with 2-AB-labeled species, 2-AA-labeled DSLNT generated fewer cross-ring fragments (four compared with five), suggesting that the nature of the reducing end substitute affects EDD fragmentation behavior.

3.2 Sialylated *N*-glycan

IRMPD and EDD of the fluorescently labeled di-sialylated *N*-glycan from human transferrin were also examined (Fig. 4 and Supporting Information Fig. S1). Most product
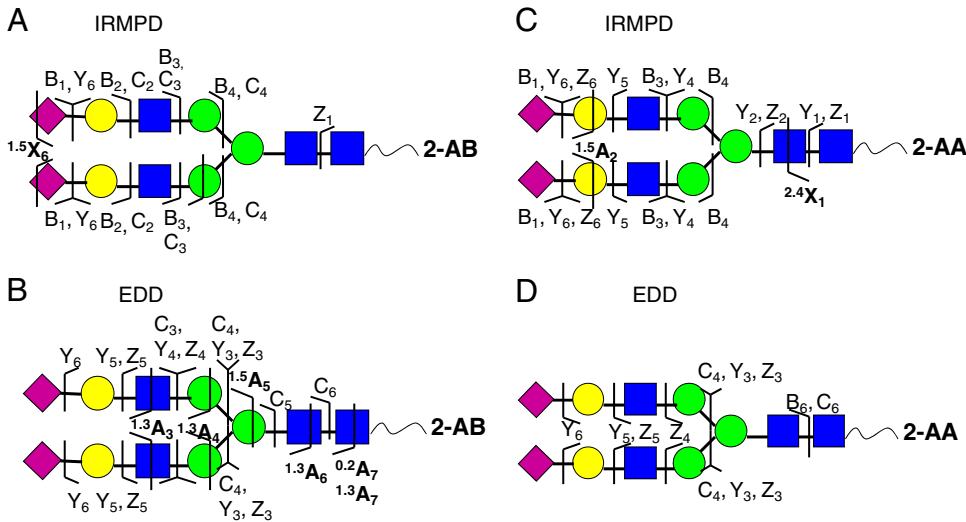
Figure 4. MS/MS of a 2-AA- (A), (B), and 2-AB- (C), (D) derivatized *N*-linked glycan released from human transferrin. Fragmentation patterns from IRMPD (A), (C) and EDD (B), (D) are shown.

ions from IRMPD of the 2-AB-labeled glycan (Fig. 4A) were singly charged, whereas one product from cross-ring cleavage ($m/z = 1130.9$) was doubly charged. Most glycosidic fragments were B- and C-type ions containing the nonreducing end. EDD of the 2-AB-labeled *N*-glycan produced a large number of glycosidic and cross-ring fragments, which provided rich structural information (Fig. 4B). In addition to glycosidic cleavages between every neighboring monosaccharide, three cross-ring cleavages were observed, including ^{1,3}A-, ^{1,5}A-, and ^{0,2}A-type ions. ^{0,2}A-, ^{1,3}A-, and ^{1,5}A-type ions have been previously reported from MS/MS of deprotonated 2-AB-labeled neutral *N*-glycans in MALDI-TOF/TOF analysis [63], and such product ions are also commonly observed in negative-ion mode CAD of glycans [80–82]. The ^{1,5}A$_5$ ion ($m/z = 1769.6$) at the branching mannose of the chitobiose core aided the determination of the positions of the two antenna. Unlike EDD of 2-AA- and 2-AB-labeled DSLNT, no X-type ions were found.

MS/MS of the 2-AA-tagged *N*-glycan showed somewhat different fragmentation behavior compared with the 2-AB-tagged species. IRMPD of the 2-AA-labeled *N*-glycan resulted in efficient fragmentation, generating eleven glycosidic and two cross-ring cleavages (Fig. 4C). It is interesting to note that ^{2,4}X$_1$ containing the fluorescent tag ($m/z = 484.2$) was observed. Typically, X-type ions are absent in CAD/ IRMPD of *N*-glycans [18, 83]. The observation of X-type ions following derivatization may indicate that the charge locations are different in the 2-AA-labeled *N*-glycan compared with the underivatized glycan. Introduction of the acidic tag 2-AA adds an additional likely site for deprotonation. EDD of the 2-AA-labeled *N*-glycan resulted only in glycosidic cleavages (Fig. 4D). All observed Y- and Z-type ions contained the fluorescent label 2-AA, suggesting that one negative charge is located on 2-AA. Compared with EDD of the 2-AB-labeled *N*-glycan, the most distinct difference was the absence of cross-ring fragments. This difference may be

explained by the altered charge location (as further discussed below).

3.3 LSTb

LSTb is a branched mono-sialylated oligosaccharide with the composition Galβ3(Neu5Acβ6)GlcNAcβ3Galβ4Glc. Negative-ion mode IRMPD and EDD of 2-AA-labeled LSTb were investigated and the results are shown in Fig. 5. IRMPD of 2-AA-labeled LSTb (Fig. 5A) yielded a complete series of Y- and Z-ions and also one cross-ring fragment (^{0,2}X$_{3\alpha}$). Again, all the Y- and Z-type ions contained the fluorescent tag. EDD of 2-AA-labeled LSTb (Fig. 5B) produced six additional glycosidic and two additional cross-ring fragments, including ^{1,5}X$_2$ and ^{1,5}X$_{3\beta}$ ions. ^{0,2}X- and ^{1,5}X-type ions have also been reported in positive-ion mode high-energy CAD, laser-induced dissociation of sodiated 2-AB-labeled oligosaccharides, and EDD of sialylated oligosaccharides [34, 63, 69]. Similar to EDD of 2-AA-labeled DSLNT and the *N*-glycan, unique product ions such as neutral loss (H_2O and CH_3O) from the charge reduced species and C−2 H type satellite ions were observed in the EDD spectrum.

2-AB labeling of LSTb was also conducted and the labeling reaction was successful; however, even with careful tuning of the instrument parameters, the signal abundance of doubly charged species was too low for EDD. Therefore, we were not able to investigate EDD of 2-AB-labeled LSTb. In EDD, at least two precursor ion charges are required. In addition, due to the low efficiency of EDD [27], abundant precursor ion signal is a prerequisite to observe product ions. LSTb has only one acidic site, which is the carboxylic acid on the sialic acid and 2-AB is a neutral tag that does not enhance ionization in negative-ion mode. In contrast, 2-AA-labeled LSTb readily generated abundant signal in MS due to the acidity of 2-AA, thus EDD fragmentation could easily
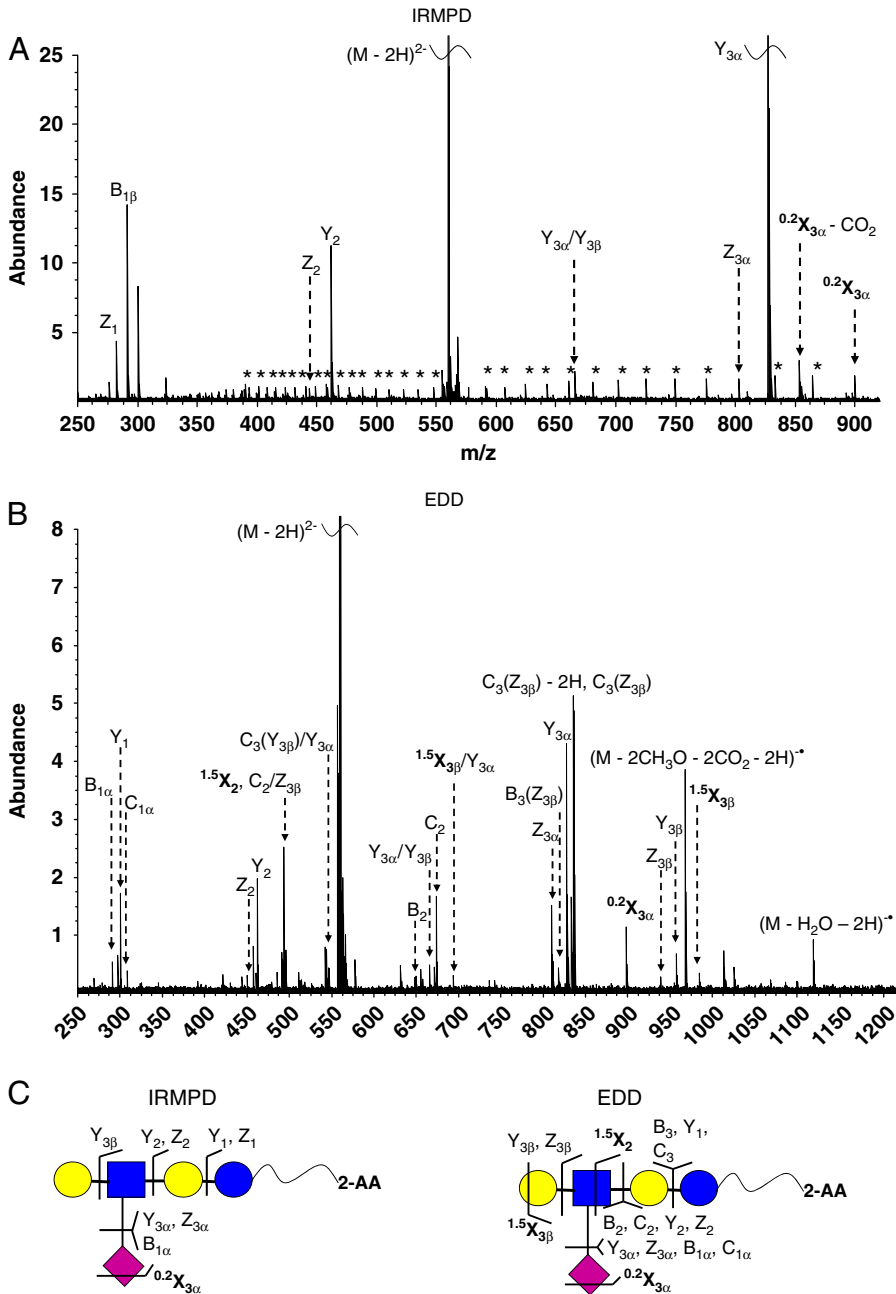
Figure 5. (A) IRMPD (80 scans, 1 s at 10 W) and (B) EDD (80 scans, 1 s irradiation, cathode bias, −30 V) spectra of doubly deprotonated 2-AA-labeled LSTb ($m/z = 558.69$). Cross-ring fragments are highlighted in bold, reducing end fragment ions lacking 2-AA are underlined in the spectra, and electronic noise peaks are indicated by asterisks. All product ions are singly charged. Fragmentation patterns from IRMPD and EDD are shown in (C).

be achieved. These observations suggest that the chosen fluorescent tag for derivatization has a strong influence on whether EDD will be successful.

3.4 Influence of reducing end derivatization on EDD fragmentation

EDD fragmentation patterns of DSLNT, LSTb, and the *N*-linked glycan released from human transferrin with and without fluorescent labels are summarized in Table 1. Although product ions resulting from glycosidic and cross-

ring cleavages were observed in almost all cases, the degree of fragmentation was different, particularly for the number of observed cross-ring cleavages. Underivatized oligosaccharides provided the most cross-ring fragments in all three sialylated oligosaccharides investigated, followed by 2-AB-labeled oligosaccharides. This result is similar to the previous studies reported by Harvey and coworkers in positive-ion mode [69]. The latter authors compared the effects of reducing end substituent in high-energy CAD of *N*-linked oligosaccharides, including underivatized and 2-AB-labeled oligosaccharides, and *N*-glycopeptides with one and four amino acids. Compared with 2-AB-derivatized

Table 1. EDD fragmentation summary of DSLNT, LSTb, and an *N*-glycan released from transferrin with or without fluorescent labels

EDD fragmentation	DSLNT	LSTb	*N*-Glycan from transferrin
Unlabeled	10 Glycosidic	11 Glycosidic	16 Glycosidic
	6 Cross-ring	7 Cross-ring	5 Cross-ring
2-AA labeled	13 Glycosidic	13 Glycosidic	10 Glycosidic
	4 Cross-ring	3 Cross-ring	0 Cross-ring
2-AB labeled	11 Glycosidic	N/A	11 Glycosidic
	5 Cross-ring		3 Cross-ring

oligosaccharides, the native species generated a more complete series of glycosidic fragments and also more cross-ring fragments due to the open nature of the reducing terminus ring [69].

2-AA labeling enhances signal abundance of oligosaccharides in negative-ion mode; however, the 2-AA-derivatized oligosaccharides generated the smallest number of cross-ring cleavages. Particularly, no cross-ring fragments were observed for the 2-AA-labeled *N*-glycan (compared with three from the 2-AB-labeled species and five from the native glycan), which makes 2-AA labeling less favorable in EDD of derivatized oligosaccharides. One possible explanation of this observation is that the introduction of a fluorescent tag at the reducing end of oligosaccharides alters the locations of the negative charges. It has been previously reported that deprotonated hydroxyl is required to obtain cross-ring cleavages in negative-ion mode [80–82]. Without derivatization, it is most favorable for the negative charges to be located on the sialic acids, but also possible to have deprotonated hydroxyl groups. When 2-AA is introduced at the reducing end, the carboxylic acid on 2-AA is preferably deprotonated, which competes with deprotonation of hydroxyl groups, thus making cross-ring cleavages less likely to occur. 2-AB is a neutral fluorescent label; therefore, introduction of 2-AB does not alter the location of negative charges. However, for less acidic oligosaccharides, which are difficult to doubly deprotonate, 2-AB is less favorable due to the lack of an acidic moiety.

4 Concluding remarks

We demonstrate that EDD of fluorescently labeled sialylated oligosaccharides results in extensive fragmentation, providing rich glycosidic and cross-ring fragments. We also show that complementary structural information can be obtained from EDD compared with IRMPD of the same species. When investigating the influence of introducing different fluorescent labels at the reducing end of oligosaccharides, we found that not only do the labels affect signal abundance, but they also have a strong influence on the EDD fragmentation behavior. Native oligosaccharides showed the most extensive fragmentation compared with their 2-AA- and 2-AB-labeled counterparts. The acidic tag 2-AA promotes precursor ion signal abundance in negative-ion

mode. However, it introduces another deprotonation site to compete with the sialic acids and hydroxyl groups, thus suggesting that deprotonated hydroxyls are important for cross-ring fragmentation in EDD, as in CAD [80–82]. The neutral label 2-AB does not significantly impede the generation of cross-ring cleavages, but for small and less acidic glycans, which are difficult to doubly deprotonate, 2-AB may not be the best choice.

The authors have declared no conflict of interest.

5 References

[1] Varki, A., *Glycobiology* 1993, *3*, 97–130.

[2] Kim, Y. J., Varki, A., *Glycoconj. J.* 1997, *14*, 569–576.

[3] Raman, R., Raguram, S., Venkataraman, G., Paulson, J. C., Sasisekharan, R., *Nat. Methods* 2005, *2*, 817–824.

[4] Dube, D. H., Bertozzi, C. R., *Nat. Rev. Drug Discov.* 2005, *4*, 477–488.

[5] Bertozzi, C. R., Kiessling, L. L., *Science* 2001, *291*, 2357–2364.

[6] Finkelstein, J., *Nature* 2007, *446*, 999.

[7] Varki, A., *Nature* 2007, *446*, 1023–1029.

[8] Morelle, W., Michalski, J. C., *Curr. Pharm. Des.* 2005, *11*, 2615–2645.

[9] Zaia, J., *Chem. Biol.* 2008, *15*, 881–892.

[10] Krishnamoorthy, L., Mahal, L. K., *ACS Chem. Biol.* 2009, *4*, 715–732.

[11] Mechref, Y., Novotny, M. V., *Chem. Rev.* 2002, *102*, 321–369.

[12] Marshall, A. G., Hendrickson, C. L., Jackson, G. S., *Mass Spectrom. Rev.* 1998, *17*, 1–35.

[13] Park, Y. M., Lebrilla, C. B., *Mass Spectrom. Rev.* 2005, *24*, 232–264.

[14] Marshall, A. G., Hendrickson, C. L., *Annu. Rev. Anal. Chem.* 2008, *1*, 579–599.

[15] Harvey, D. J., *J. Mass Spectrom.* 2005, *40*, 642–653.

[16] Sagi, D., Peter-Katalinic, J., Conradt, H. S., Nimtz, M., *J. Am. Soc. Mass. Spectrom.* 2002, *13*, 1138–1148.

[17] Zaia, J., Miller, M. J. C., Seymour, J. L., Costello, C. E., *J. Am. Soc. Mass. Spectrom.* 2007, *18*, 952–960.

[18] Lancaster, K. S., An, H. J., Li, B. S., Lebrilla, C. B., *Anal. Chem.* 2006, *78*, 4990–4997.

[19] Xie, Y. M., Lebrilla, C. B., *Anal. Chem.* 2003, *75*, 1590–1598.

[20] Zhang, J. H., Schubothe, K., Li, B. S., Russell, S., Lebrilla, C. B., *Anal. Chem.* 2005, *77*, 208–214.

[21] Harvey, D. J., Naven, T. J. P., Kuster, B., Bateman, R. H., Green, M. R., Critchley, G., *Rapid Commun. Mass Spectrom.* 1995, *9*, 1556–1561.

[22] Harvey, D. J., Bateman, R. H., Green, M. R., *J. Mass Spectrom.* 1997, *32*, 167–187.

[23] Lewandrowski, U., Resemann, A., Sickmann, A., *Anal. Chem.* 2005, *77*, 3274–3283.

[24] Zhao, C., Xie, B., Chan, S. Y., Costello, C. E., O'Connor, P. B., *J. Am. Soc. Mass. Spectrom.* 2008, *19*, 138–150.

[25] Adamson, J. T., Håkansson, K., *Anal. Chem.* 2007, *79*, 2901–2910.

[26] Budnik, B. A., Haselmann, K. F., Elkin, Y. N., Gorbach, V. I., Zubarev, R. A., *Anal. Chem.* 2003, *75*, 5994–6001.

[27] McFarland, M. A., Marshall, A. G., Hendrickson, C. L., Nilsson, C. L., Fredman, P., Mansson, J. E., *J. Am. Soc. Mass. Spectrom.* 2005, *16*, 752–762.

[28] Liu, H., Håkansson, K., *Int. J. Mass Spectrom.* 2011 in press, doi: 10.1016/j.ijms.2010.10.030.

[29] Wolff, J. J., Chi, L. L., Linhardt, R. J., Amster, I. J., *Anal. Chem.* 2007, *79*, 2015–2022.

[30] Wolff, J. J., Laremore, T. N., Busch, A. M., Linhardt, R. J., Amster, I. J., *J. Am. Soc. Mass. Spectrom.* 2008, *19*, 294–304.

[31] Wolff, J. J., Laremore, T. N., Busch, A. M., Linhardt, R. J., Amster, I. J., *J. Am. Soc. Mass. Spectrom.* 2008, *19*, 790–798.

[32] Wolff, J. J., Amster, I. J., Chi, L. L., Linhardt, R. J., *J. Am. Soc. Mass. Spectrom.* 2007, *18*, 234–244.

[33] Wolff, J. J., Laremore, T. N., Leach, F. E., Linhardt, R. J., Amster, I. J., *Eur. J. Mass Spectrom.* 2009, *15*, 275–281.

[34] Adamson, J. T., Håkansson, K., *J. Am. Soc. Mass. Spectrom.* 2007, *18*, 2162–2172.

[35] Wolff, J. J., Leach, F. E., Laremore, T. N., Kaplan, D. A., Easterling, M. L., Linhardt, R. J., Amster, I. J., *Anal. Chem.* 2010, *82*, 3460–3466.

[36] Devakumar, A., Thompson, M. S., Reilly, J. P., *Rapid Commun. Mass Spectrom.* 2005, *19*, 2313–2320.

[37] Devakumar, A., Mechref, Y., Kang, P., Novotny, M. V., Reilly, J. P., *J. Am. Soc. Mass. Spectrom.* 2008, *19*, 1027–1040.

[38] Devakumar, A., Mechref, Y., Kang, P., Novotny, M. V., Reilly, J. P., *Rapid Commun. Mass Spectrom.* 2007, *21*, 1452–1460.

[39] Gao, D., Zhou, W., Håkansson, K., *58th ASMS Conference on Mass Spectrometry and Allied Topics*, Salt Lake City, Utah 2010.

[40] Brodbelt, J. S., Wilson, J. J., *Mass Spectrom. Rev.* 2009, *28*, 390–424.

[41] Eyler, J. R., *Mass Spectrom. Rev.* 2009, *28*, 448–467.

[42] Budnik, B. A., Haselmann, K. F., Zubarev, R. A., *Chem. Phys. Lett.* 2001, *342*, 299–302.

[43] Zubarev, R. A., *Mass Spectrom. Rev.* 2003, *22*, 57–77.

[44] Zhou, W., Håkansson, K., *57th ASMS Conference on Mass Spectrometry and Allied Topics*, Philadelphia, PA 2009.

[45] Wolff, J. J., Laremore, T. N., Aslam, H., Linhardt, R. J., Amster, I. J., *J. Am. Soc. Mass. Spectrom.* 2008, *19*, 1449–1458.

[46] Yoshino, K., Takao, T., Murata, H., Shimonishi, Y., *Anal. Chem.* 1995, *67*, 4028–4031.

[47] Lamari, F. N., Kuhn, R., Karamanos, N. K., *J. Chromatogr. B* 2003, *793*, 15–36.

[48] Lattova, E., Snovida, S., Perreault, H., Krokhin, O., *J. Am. Soc. Mass Spectrom.* 2005, *16*, 683–696.

[49] Anumula, K. R., *Anal. Biochem.* 2006, *350*, 1–23.

[50] Ruhaak, L. R., Zauner, G., Huhn, C., Bruggink, C., Deelder, A. M., Wuhrer, M., *Anal. Bioanal. Chem.* 2010, *397*, 3457–3481.

[51] Wuhrer, M., Deelder, A. M., Hokke, C. H., *J. Chromatogr. B* 2005, *825*, 124–133.

[52] Bowman, M. J., Zaia, J., *Anal. Chem.* 2007, *79*, 5777–5784.

[53] Xia, B. Y., Feasley, C. L., Sachdev, G. P., Smith, D. F., Cummings, R. D., *Anal. Biochem.* 2009, *387*, 162–170.

[54] Prien, J. M., Prater, B. D., Qin, Q., Cockrill, S. L., *Anal. Chem.* 2010, *82*, 1498–1508.

[55] Bigge, J. C., Patel, T. P., Bruce, J. A., Goulding, P. N., Charles, S. M., Parekh, R. B., *Anal. Biochem.* 1995, *230*, 229–238.

[56] Maslen, S., Sadowski, P., Adam, A., Lilley, K., Stephens, E., *Anal. Chem.* 2006, *78*, 8491–8498.

[57] Maslen, S. L., Goubet, F., Adam, A., Dupree, P., Stephens, E., *Carbohydr. Res.* 2007, *342*, 724–735.

[58] Wuhrer, M., Koeleman, C. A. M., Deelder, A. M., *Anal. Chem.* 2009, *81*, 4422–4432.

[59] Harvey, D. J., *Analyst* 2000, *125*, 609–617.

[60] Harvey, D. J., *J. Am. Soc. Mass. Spectrom.* 2000, *11*, 900–915.

[61] Sato, Y., Suzuki, M., Nirasawa, T., Suzuki, A., Endo, T., *Anal. Chem.* 2000, *72*, 1207–1216.

[62] Wuhrer, M., Koeleman, C. A. M., Hokke, C. H., Deelder, A. M., *Int. J. Mass Spectrom.* 2004, *232*, 51–57.

[63] Wuhrer, M., Deelder, A. M., *Anal. Chem.* 2005, *77*, 6954–6959.

[64] Morelle, W., Slomianny, M. C., Diemer, H., Schaeffer, C., van Dorsselaer, A., Michalski, J. C., *Rapid Commun. Mass Spectrom.* 2005, *19*, 2075–2084.

[65] Chen, X. Y., Flynn, G. C., *J. Am. Soc. Mass. Spectrom.* 2009, *20*, 1821–1833.

[66] Takegawa, Y., Deguchi, K., Ito, S., Yoshioka, S., Nakagawa, H., Nishimura, S. I., *Rapid Commun. Mass Spectrom.* 2005, *19*, 937–946.

[67] Deguchi, K., Takegawa, Y., Ito, H., Miura, N., Yoshioka, S., Nagai, S., Nakagawa, H., Nishimura, S. I., *Rapid Commun. Mass Spectrom.* 2006, *20*, 412–418.

[68] Briggs, J. B., Keck, R. G., Ma, S., Lau, W. D., Jones, A. J. S., *Anal. Biochem.* 2009, *389*, 40–51.

[69] Kuster, B., Naven, T. J. P., Harvey, D. J., *Rapid Commun. Mass Spectrom.* 1996, *10*, 1645–1651.

[70] Wilson, J. J., Brodbelt, J. S., *Anal. Chem.* 2008, *80*, 5186–5196.

[71] Morelle, W., Page, A., Michalski, J. C., *Rapid Commun. Mass Spectrom.* 2005, *19*, 1145–1158.

[72] Yang, J., Mo, J. J., Adamson, J. T., Håkansson, K., *Anal. Chem.* 2005, *77*, 1876–1882.

[73] Tsybin, Y. O., Witt, M., Baykut, G., Kjeldsen, F., Hakansson, P., *Rapid Commun. Mass Spectrom.* 2003, *17*, 1759–1768.

[74] Caravatti, P., Allemann, M., *Org. Mass Spectrom.* 1991, *26*, 514–518.

[75] Yang, J., Håkansson, K., *Int. J. Mass Spectrom.* 2008, *276*, 144–148.

[76] Senko, M. W., Canterbury, J. D., Guan, S. H., Marshall, A. G., *Rapid Commun. Mass Spectrom.* 1996, *10*, 1839–1844.

[77] Ledford, E. B., Rempel, D. L., Gross, M. L., *Anal. Chem.* 1984, *56*, 2744–2748.

[78] Lohmann, K. K., von der Lieth, C. W., *Nucleic Acids Res.* 2004, *32*, W261–W266.

[79] Domon, B., Costello, C. E., *Glycoconj. J.* 1988, *5*, 397–409.

[80] Harvey, D. J., *J. Am. Soc. Mass Spectrom.* 2005, *16*, 622–630.

[81] Harvey, D. J., *J. Am. Soc. Mass Spectrom.* 2005, *16*, 631–646.

[82] Harvey, D. J., *J. Am. Soc. Mass Spectrom.* 2005, *16*, 647–659.

[83] Pikulski, M., Hargrove, A., Shabbir, S. H., Anslyn, E. V., Brodbelt, J. S., *J. Am. Soc. Mass Spectrom.* 2007, *18*, 2094–2106.